





RESEARCH ARTICLE

WILEY

Human metabolism and basic pharmacokinetic evaluation of AP-238: A recently emerged acylpiperazine opioid

Pietro Brunetti^{1,2}  | Diletta Berardinelli^{1,2} | Arianna Giorgetti^{2,3} | Hannes Max Schwelm^{2,4}  | Belal Haschimi^{2,4}  | Susi Pelotti³ | Francesco Paolo Busardò¹ | Volker Auwärter² 

¹Unit of Forensic Toxicology, Section of Legal Medicine, Department of Biomedical Sciences and Public Health, Marche Polytechnic University, Ancona, Italy

²Institute of Forensic Medicine, Forensic Toxicology, Medical Center – University of Freiburg, Faculty of Medicine, University of Freiburg, Germany

³Unit of Legal Medicine, Department of Medical and Surgical Sciences, University of Bologna, Bologna, Italy

⁴Hermann Staudinger Graduate School, University of Freiburg, Freiburg, Germany

Correspondence

Arianna Giorgetti, Institute of Forensic Medicine, Forensic Toxicology, Medical Center – University of Freiburg, Faculty of Medicine, University of Freiburg, Germany.
Email: arianna.giorgetti@unibo.it

Abstract

As a consequence of recently implemented legal restrictions on fentanyl analogs, a new generation of acylpiperazine opioids appeared on the illicit drug market. AP-238 was the latest opioid in this series to be notified by the European Early Warning System in 2020 and was involved in an increasing number of acute intoxications. AP-238 metabolism was investigated to provide useful markers of consumption. For the tentative identification of the main phase I metabolites, a pooled human liver microsome assay was performed. Further, four whole blood and two urine samples collected during post-mortem examinations and samples from a controlled oral self-administration study were screened for anticipated metabolites. In total, 12 AP-238 phase I metabolites were identified through liquid chromatography-quadrupole time-of-flight mass spectrometry in the *in vitro* assay. All of these were confirmed *in vivo*, and additionally, 15 phase I and five phase II metabolites were detected in the human urine samples, adding up to a total of 32 metabolites. Most of these metabolites were also detected in the blood samples, although mostly with lower abundances. The main *in vivo* metabolites were built by hydroxylation combined with further metabolic reactions such as *O*-methylation or *N*-deacylation. The controlled oral self-administration allowed us to confirm the usefulness of these metabolites as proof of intake in abstinence control. The detection of metabolites is often crucial to documenting consumption, especially when small traces of the parent drug can be found in real samples. The *in vitro* assay proved to be suitable for the prediction of valid biomarkers of novel synthetic opioid intake.

KEYWORDS

high resolution mass spectrometry, human liver microsomes, novel synthetic opioid, urinary biomarkers

This is an open access article under the terms of the [Creative Commons Attribution](https://creativecommons.org/licenses/by/4.0/) License, which permits use, distribution and reproduction in any medium, provided the original work is properly cited.

© 2023 The Authors. *Drug Testing and Analysis* published by John Wiley & Sons Ltd.

1 | INTRODUCTION

The phenomenon of new psychoactive substances (NPS) is constantly evolving, with novel synthetic opioids (NSOs) representing a fast-growing subclass.¹ Since their introduction into the illegal drug market, NSOs have been misused in place of heroin, gaining popularity due to their cheaper cost and ease of concealment and transport. NSOs are manufactured and sold as powders, liquids, tablets and capsules, or, more recently, as liquids for e-cigarettes or in the form of infused papers.^{2–4} It was postulated that NSOs mainly act as selective μ -opioid receptor (MOR) agonists, displaying various degrees of potency and efficacy, most of them being more potent than morphine, entailing a higher risk of overdose.^{5,6} Adverse effects reported after NSO intake include nausea, hypothermia, sedation, drowsiness, and respiratory depression.⁷ So far, 73 compounds belonging to different classes of basic chemical structures have been reported to the European Monitoring Center for Drugs and Drug Addiction (EMCDDA).^{4,5} Since 2012, fentanyl and its analogs (FAs) have ruled the illegal opioid market, contributing to the “opioid epidemic crisis” with more than 130,000 deaths in North America.^{8,9} Meanwhile, in some parts of Europe, owing to a shortage in the availability of classical opioids, FAs have established themselves as the most trafficked NSOs.^{10,11} However, because of recent legal restrictions made to contain their spread, the number of FAs drastically decreased from 2017 onward.¹² At the same time, non-fentanyl NSOs increasingly emerged on the drug market.^{6,13} Among these, the class of acylpiperazines (APs) is of rising concern, as testified by recent forensic toxicological findings.^{14,15}

In contrast to FAs, the chemical structure of APs is characterized by a piperazine core and a cinnamyl moiety instead of the piperidine and the phenethyl chain (Figure 1). The prototype of this structural class is AP-237 (IUPAC name: 1-[4-[(2E)-3-phenylprop-2-en-1-yl]piperazine-1-yl]butan-1-one), also known as bucinnazine. First synthesized in 1968, AP-237 was found to be a potent analgesic in animal models with better oral efficacy and less dependence liability than morphine.^{16–18} In China, AP-237 is an approved drug used as a moderate intensity analgesic for patients suffering from migraine, traumatic pain, trigeminal neuralgia, and cancer-related pain, but it has so far not been approved for medical use elsewhere.^{19,20} In 2020, the 2,6-dimethyl propionyl analog of AP-237, namely AP-238 (IUPAC name: 1-[2,6-dimethyl-4-[(2E)-3-phenylprop-2-en-1-yl]piperazine-1-yl]propan-1-one), started to circulate via Internet shops and was

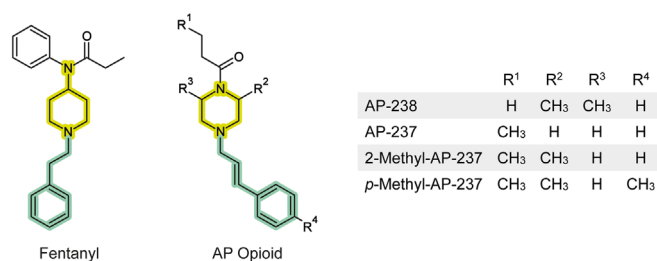


FIGURE 1 Acylpiperazine (AP) opioids in comparison to fentanyl.

involved in a case of fatal intoxication.^{21,22} Despite the long (pre)clinical history of AP compounds, deeper knowledge concerning their pharmacological and toxicological properties is still lacking in the available literature. In 1968, Cigarella et al. synthesized a series of compounds structurally related to the analgetic 8-acyl-3,8-diazabicyclo [3.2.1]octanes, with AP-238 (compound VII in the reference) being about two times more potent than morphine with regard to analgesia and acute toxicity in rodents, with a shorter duration of action.²³ More recently, Fogarty et al. characterized a wide panel of NSOs using an in vitro MOR activation assay. AP-238 resulted as the most potent drug in this subclass with an EC₅₀ of 248 nM, 95% CI: 184–333 nM (hydromorphone: EC₅₀ of 26.9 nM, 95% CI: 19.9–36.4 nM), but was considerably less potent than fentanyl.^{6,24} Limited data are also available regarding the metabolism of APs. Preliminary studies on APs showed that the main metabolites are formed via *N*-deacylation, hydroxylation, and combinations thereof. It has also been speculated that APs could undergo similar metabolic reactions, like MT-45, AD-1211, and other compounds bearing a piperazine ring.²⁵ Therefore, the aim of this study was the characterization of phase I metabolites of AP-238 using in vitro incubations with pooled human liver microsomes (pHLMs) and real samples by means of liquid chromatography coupled to high-resolution mass spectrometry (LC–HRMS). Finally, the most reliable urinary markers were evaluated performing a controlled oral self-administration study.

2 | MATERIALS AND METHODS

2.1 | Chemicals and reagents

Formic acid (Rotipuran[®] ≥98%, p.a.), sodium hydroxide (≥99%, p.a., pellets), and potassium hydrogen phosphate (≥99%, p.a.) were obtained from Carl Roth (Karlsruhe, Germany). Acetonitrile (ACN, LC–MS grade) and ammonium formate 10 M (99.995%) were bought from Sigma-Aldrich (Steinheim, Germany). Isopropanol (Prepsolv[®]) was obtained from Merck (Darmstadt, Germany). Acetic acid glacial (USP, EP, and JP grades) was purchased from VWR (Darmstadt, Germany). pHLMs (50 donors, 20 mg/mL protein in 250 mM sucrose), NADPH-regenerating Solutions A and B (reductase activity 0.43 μ mol/min^{*}mL), and potassium phosphate buffer 0.5 M (pH 7.5) were purchased from Corning (New York, USA). NADPH regenerating Solution A consisted of 26 mM NADP⁺, 66 mM glucose-6-phosphate, and 66 mM MgCl₂ in water. NADPH-regenerating Solution B consisted of 40 U/mL glucose-6-phosphate dehydrogenase in 5 mM sodium citrate. Merck (Darmstadt, Germany) produced the β -glucuronidase/aryl-sulfatase (*Helix pomatia*) used for conjugate cleavage.

AP-238 HCl (purity ≥98%) was provided as hydrochloride from Cayman Chemical (Ann Arbor, MI, USA). Full analytical data (GC–MS, NMR, and FTIR) on the structural characterization of AP-238 have already been provided.²² Deionized water was prepared using a Medica[®] Pro deionizer from ELGA (Celle, Germany). Blank urine samples were donated by a volunteer and tested for the absence of AP-238 metabolites prior to use. Mobile phase A (1% ACN, 0.1% HCOOH,

and 2 mM $\text{NH}_4^+\text{HCOO}^-$ in water) and mobile phase B (0.1% HCOOH and 2 mM $\text{NH}_4^+\text{HCOO}^-$ in ACN) were freshly prepared prior to analysis. The sodium formate/acetate clusters solution, used for external and internal mass calibration of the QToF-MS instrument, was prepared by mixing 250 mL deionized water, 250 mL isopropanol, 750 μL acetic acid, 250 μL formic acid, and 500 μL sodium hydroxide 1 M.

2.2 | pHLM assay

In vitro phase I metabolites of AP-238 were tentatively generated by applying a pHLM assay, which was performed by adding 0.5 μL of a 1 mg/mL reference standard solution (final concentration of 10 $\mu\text{g}/\text{mL}$ in ACN) to 49.5 μL of a reaction mixture consisting of 2.5 μL pHLM, 2.5 μL NADPH-regenerating Solution A, 0.5 μL NADPH regenerating Solution B, 10 μL phosphate buffer 0.5 M (pH 7.4), and 34 μL deionized water. The reaction was performed during a 2 h-long incubation at 37°C and was terminated by the addition of 150 μL ice-cold ACN. Preliminary tests with shorter incubation times (0.5 and 1 h) resulted in less complete metabolic profiles and lower turnover. After the addition of 25 μL of a 10 M ammonium formate solution, the sample was centrifuged for 4 min at 13,000 rpm. Then, the organic layer was transferred into a separate vial. For LC-QToF-MS analysis (parameters described in Section 2.4), 30 μL of the extracts was evaporated to dryness under a stream of nitrogen and reconstituted with 30 μL of mobile phase A/B (95/5, v/v). Two blank pHLM samples, one containing no reference standard (zero-control) and the other one containing no pHLM-enzymes (blank-control), were processed accordingly and served as negative controls. The experiments were performed in triplicates.

2.3 | Self-administration study

For the investigation of the in vivo metabolism, a volunteer (Caucasian male, 29 years old, 72 kg body weight) ingested one gelatine capsule containing AP-238 (1.19 mg). The amount of the drug was extrapolated from previous pharmacological studies and after consulting self-assessment online fora to minimize the risk of adverse effects.^{6,24} One serum and one urine sample were taken before ingestion of the drug, and four serum samples (30 min, 1, 2, and 24 h post intake) as well as six urine samples (30 min, 1, 4, 7, 23, and 96 h post intake) were taken. All samples were stored at -20°C until analysis. Approval by an ethics committee is not required for self-experiments in Germany.

2.4 | Human urine and blood preparation

For the investigation of the in vivo AP-238 phase I main metabolites, two urine samples and four whole blood samples from four forensic toxicological routine cases were analyzed. Sample preparation was conducted as previously described, with minor modifications.²⁶ After

addition of 100 μL phosphate buffer (pH 6) and 10 μL β -glucuronidase/aryl-sulfatase to 100 μL of urine/blood, the samples were incubated at 45°C (1 h). Afterwards, 1 mL of ice-cold ACN and 100 μL of a 10 M ammonium formate solution were added. The mixture was shaken (overhead mixing) for 5 min, then centrifuged for 10 min at 14,000 rpm (Heraeus Megafuge 1.0, Thermo Scientific, Schwerte, Germany). One milliliter of the organic layer was then transferred into a separate vial and evaporated to dryness under a stream of nitrogen. Finally, the samples were reconstituted in 50 μL of mobile phase A/B (95/5, v/v) prior to LC-QToF-MS analysis (Section 2.5). Negative control samples (blank urine) were prepared accordingly. Serum and urine samples collected after the controlled self-administration study were submitted to the same sample preparation procedure.

2.5 | Identification of tentative main metabolites (LC-QToF-MS)

LC-QToF-MS analysis was performed on an Impact II QToF instrument coupled with an Elute RS HPLC system (Bruker Daltonik, Bremen, Germany). Chromatographic separation was performed on a Kinetex® C18 column (2.6 μm , 100 Å, 100, 2.1 mm; Phenomenex, Aschaffenburg, Germany). Gradient elution was 0 min, 5%B; 1 min, 5%B; 8 min, 15%B; 12 min, 30%B; 14 min, 65%B; 15 min, 95%B held for 2 min; 17.1–20 min gradual return to initial condition. The flow rate was set to 0.5 mL/min. The autosampler and column oven temperature were set to 10 and 40°C, respectively. The injection volume was 5 μL . HyStar™ ver. 3.2 and DataAnalysis (DA) ver. 4.2 (Bruker Daltonik, Bremen, Germany) were used for data acquisition and processing, respectively.

The MS was operated in positive electrospray ionization (ESI^+) mode, acquiring spectra in the m/z range of 50–650. The dry gas temperature was set to 200°C with a dry gas flow of 8.0 L/min. The nebulizer gas pressure was 2 bars. Full scan and auto MS^2 data were acquired in one run at an acquisition rate of 4.0 Hz. In a second run, full scan and broadband collision-induced dissociation (bbCID) data were acquired to screen for additional metabolites and to prevent missing product ion spectra of minor metabolites during auto MS^2 scan. The resulting spectra were compared with a list of hypothetical metabolites based on the known biotransformation reactions of structurally similar NSOs.^{19,27} The resulting hits for the molecular ions of anticipated metabolites were further analyzed with defined quadrupole mass selection (± 0.5 Da) and retention time windows. All identified molecular ions of the metabolites were added to a scheduled precursor ion list (SPL) and further characterized in MS^2 mode to produce product ion spectra.

Additionally, the maximum number of MS^2 cycles that were performed on a precursor ion was set to the value of three (“active exclusion”). If a precursor exceeded this number of cycles, the molecular ion was excluded from further analysis for 1.0 min. Using this workflow, pure product ion spectra of even low-abundant metabolites can be obtained, even if they co-elute with highly abundant metabolites or highly abundant signals originating from the matrix. The collision

energy applied for bbCID was 30 ± 6 eV. Full scan and MS² data were acquired at an acquisition rate of 2.0 Hz in one run. Nitrogen was used as a collision gas. The voltages for the capillary and end plate offset were 2500 and 500 V, respectively. External and internal mass calibrations were performed using sodium formate/acetate clusters and high-precision calibration (HPC) mode.

For comparison of the relative abundances of the metabolites for human samples and pHLM assays, peak area ratios were calculated by dividing the pHLM ($n = 3$ replicates), post-mortem urine ($n = 2$ samples), and blood ($n = 4$ samples) mean peak areas of each metabolite by the peak area of the most abundant metabolite in the respective matrix. The metabolite with the highest peak area was set to 100%, and the relative abundances of all detected metabolites were ranked. The following criteria were applied for metabolite identification: mass error of the precursor ion <5 ppm, mass error of diagnostic product ions <10 ppm, signal-to-noise ratio >3:1, and matching isotope pattern.

2.6 | Semi-quantitation for basic pharmacokinetics

The calibration range and limit of detection (LOD) were determined by spiking blank serum and urine samples with AP-238 at concentrations from 1.0 to 100 ng/mL and fortifying with 10 μ L of internal standard (*O*-desmethyltramadol-D6 100 ng/mL). The LOD criteria were fulfilled for signal-to-noise ratios of at least 3:1 for the target and qualifier ions at 0.3 ng/mL. To account for heteroscedasticity, a weighted calibration model (1/ x) was applied. Selectivity, accuracy and precision were checked and found acceptable. LLOQ was set to 1.0 ng/mL. Since for the assessment of preliminary basic pharmacokinetic data semi-quantitative results were sufficient, a full method validation according to forensic guidelines was not carried out.²⁸ Analyses were performed on a Shimadzu Nexera X2 LC-30 AD (Duisburg, Germany) coupled to a QTRAP 5500 triple quadrupole linear ion trap instrument (Sciex, Darmstadt, Germany). The LC system was equipped with a Kinetex[®] F5 column (2.6 μ m, 100 \times 2.1 mm) (Phenomenex, Aschaffenburg, Germany) with a corresponding pre-column (2.1 mm) from Phenomenex. The autosampler temperature was maintained at 10°C, and the injection volume was 10 μ L. Chromatographic conditions were as follows (flow 0.5 mL/min): an initial hold at 5% B for 1 min, increased to 22.5% B at 4.5 min, then to 32.5% B at 10.75 min, then to 95%B at 13.5 min, holding at 95% B for 2 min, and then decreasing to initial conditions in 0.5 min, held for

3.5 min. Total runtime was 19.5 min. Samples were analyzed in ESI positive mode with an ion spray voltage of 4500 V. The gas settings were as follows: curtain gas 40 psi, collision gas medium, ion source gas (1) 60 psi, and ion source gas (2) 70 psi. The source temperature was set to 500°C. LC/MS parameters are displayed in [Supporting information](#) section.

3 | RESULTS AND DISCUSSION

3.1 | AP-238 human metabolism

Eluting at 8.52 min at the previously reported LC-QToF-MS conditions, AP-238 ($[M + H]^+$ at m/z 287.2118) was detected in the pHLM blank-control. The same mass and retention time were found in the real samples. The AP-238 fragmentation pattern was consistent with the scientific literature and displayed characteristic fragments at m/z 91.0542, 117.0699, and 169.1335, corresponding to the tropylium, cinnamyl, and APs moiety (Figure 2).^{21,24}

After enzymatic cleavage of glucuronides and sulfates, the analysis of the human phase I metabolism led to the detection of 32 metabolites in urine and 26 in blood, assigned to the following biotransformations: mono and dihydroxylation, *N*-deacylation, dihydrodiol formation, oxidation, and combination thereof (Table 1, Figure 3). All 12 metabolites anticipated in vitro using the pHLM assays, as well as all 26 metabolites detected in blood, were confirmed in authentic urine samples. Figure 4 shows the extracted ion chromatogram of AP-238 and metabolites from post-mortem urine (post-mortem blood and pHLM chromatograms are reported in the [Supporting information](#) section). Although the initial purpose of this study was to elucidate the AP-238 phase I metabolic pathway, five additional phase II metabolites, obtained via *O*-methylation, were also reported. In Figure 5d, the fragmentation pattern of AP-238's main metabolites, as shown in both authentic urine and blood samples, is displayed. It should be mentioned that the identification of glucuronide or sulfate metabolites was not the aim of this study.

3.1.1 | Hydroxylation(s)

M14 was the metabolite with the most intense signal in all authentic urines and the second among the detected blood metabolites. Given its protonated mass at m/z 303.2067, M14 was the result of AP-238

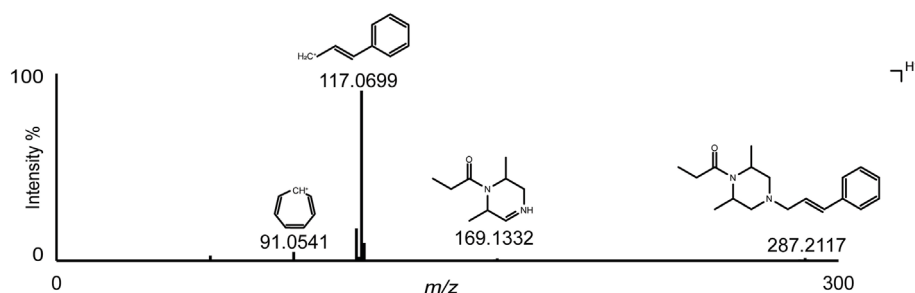


FIGURE 2 LC-qToF-MS spectrum and suggested fragmentation of AP-238.

TABLE 1 Identified in vitro and in vivo phase I metabolites of AP-238 (M00) in the order of their retention time (RT). For ranking the metabolites, relative mean area ratios (MAR) of each metabolite were calculated by comparison to the most abundant metabolite (100% in bold). For post-mortem samples, the mean of the analyzed samples was used.

ID	RT (min)	Biotransformation	Calculated [M + H] ⁺	Formula [M + H] ⁺	Mass error (ppm)	Diagnostic product ions (m/z)	Diagnostic product ions formula	Diagnostic product ions mass error (ppm)	Post-mortem urine ranking position (MAR %)	Post-mortem blood ranking position (MAR %)	pHLM ranking position (MAR %)
M00	8.52	-	287.2118	C ₁₈ H ₂₇ N ₂ O	0.7	117.0699, 169.1335	C ₉ H ₉ , C ₉ H ₁₇ N ₂ O	-0.9, -0.2	-	-	-
M01	1.17	Hydroxylation (C) + N-deacylation	247.1805	C ₁₅ H ₂₃ N ₂ O	0.2	115.123, 133.0648	C ₆ H ₁₅ N ₂ , C ₉ H ₉ O	-0.5, -0.9	9 (7.39%)	11 (3.85%)	-
M02	1.57	Hydroxylation (C) + N-deacylation	247.1805	C ₁₅ H ₂₃ N ₂ O	0.3	115.123, 133.0648	C ₆ H ₁₅ N ₂ , C ₉ H ₉ O	0.4, 0.1	31 (0.25%)	-	-
M03	2.25	DIOH (C and A)	319.2016	C ₁₈ H ₂₇ N ₂ O ₃	-0.7	115.123, 133.0648	C ₆ H ₁₅ N ₂ , C ₉ H ₉ O	-0.4, -0.6	8 (40.1%)	17 (1.4%)	-
M04	2.63	DIOH (C and A)	319.2016	C ₁₈ H ₂₇ N ₂ O ₃	0.4	115.123, 133.0648	C ₆ H ₁₅ N ₂ , C ₉ H ₉ O	-0.3, -0.5	17 (1.55%)	23 (0.4%)	10 (0.47%)
M05	3.33	DIOH (C and P) + N-deacylation	263.1754	C ₁₅ H ₂₃ N ₂ O ₂	0.3	131.1179, 133.0648	C ₆ H ₁₅ N ₂ O, C ₉ H ₉ O	-0.8, -0.6	4 (17.22%)	4 (7.9%)	7 (3.37%)
M06	3.40	DIOH (C)	319.2016	C ₁₈ H ₂₇ N ₂ O ₃	1	149.0597, 171.1492	C ₉ H ₉ O ₂ , C ₉ H ₁₉ N ₂ O	0, 0.8	11 (6.24%)	21 (0.99%)	5 (5.36%)
M07	3.44	DIOH (C and P)	319.2016	C ₁₈ H ₂₇ N ₂ O ₃	0.5	133.0648, 187.1441	C ₉ H ₉ O, C ₉ H ₁₉ N ₂ O ₂	0.2, 0.5	12 (4.71%)	20 (0.91%)	-
M08	3.64	Dihydrodiol	321.2173	C ₁₈ H ₂₉ N ₂ O ₃	1.8	183.1492, 265.1911	C ₁₅ H ₂₅ N ₂ O ₂ , C ₉ H ₁₉ N ₂ O ₂	1.7, -1.3	30 (0.26%)	23 (0.4%)	12 (0.15%)
M09	3.67	N-deacylation	231.1856	C ₁₅ H ₂₃ N ₂	0.6	91.0542, 117.0699	C ₇ H ₇ , C ₉ H ₉	1, 0.6	22 (0.77%)	9 (4.92%)	-
M10	3.71	Hydroxylation (C)	303.2067	C ₁₈ H ₂₇ N ₂ O ₂	-0.2	133.0648, 171.1492	C ₉ H ₉ O, C ₉ H ₁₉ N ₂ O	0.9, 1	18 (1.41%)	6 (5.84%)	-
M11	3.81	Dihydrodiol	321.2173	C ₁₈ H ₂₉ N ₂ O ₃	1.1	183.1492, 265.1911	C ₁₅ H ₂₅ N ₂ O ₂ , C ₉ H ₁₉ N ₂ O ₂	2.8, 0.9	19 (1.37%)	10 (4.13%)	4 (5.77%)
M12	3.99	DIOH (C) + O-methylation	333.2173	C ₁₉ H ₂₉ N ₂ O ₃	2.8	163.0754, 171.1492	C ₁₀ H ₁₁ O ₂ , C ₉ H ₁₉ N ₂ O	1, -0.2	25 (0.65%)	22 (0.52%)	-
M13	4.36	DIOH (C)	319.2016	C ₁₈ H ₂₇ N ₂ O ₃	1.4	149.0597, 171.1492	C ₉ H ₉ O ₂ , C ₉ H ₁₉ N ₂ O	1.2, 1.9	20 (1.04%)	24 (0.29%)	-
M14	4.53	Hydroxylation (C)	303.2067	C ₁₈ H ₂₇ N ₂ O ₂	1.9	133.0648, 171.1492	C ₉ H ₉ O	1, 1.7	1 (100%)	2 (70.86%)	2 (67.79%)
M15	4.74	DIOH (C and P)	319.2016	C ₁₈ H ₂₇ N ₂ O ₃	2	133.0648, 187.1441	C ₉ H ₉ O, C ₉ H ₁₉ N ₂ O ₂	0.9, 0.8	28 (0.41%)	-	-
M16	4.87	DIOH (C and P)	319.2016	C ₁₈ H ₂₇ N ₂ O ₃	1.2	133.0648, 187.1441	C ₉ H ₉ O, C ₉ H ₁₉ N ₂ O ₂	-0.2, -0.5	29 (0.29%)	-	-
M17	4.98	Hydroxylation (C)	303.2067	C ₁₈ H ₂₇ N ₂ O ₂	2.6	133.0648, 171.1492	C ₉ H ₉ O, C ₉ H ₁₉ N ₂ O	2, 1.8	15 (3.14%)	18 (1.05%)	-
M18	5.36	Hydroxylation (P)	303.2067	C ₁₈ H ₂₇ N ₂ O ₂	0.2	117.0699, 185.1285	C ₉ H ₉ , C ₉ H ₁₇ N ₂ O ₂	-0.6, -0.7	6 (44.4%)	7 (5.18%)	8 (3.35%)
M19	5.38	DIOH (C) + O-methylation	333.2173	C ₁₉ H ₂₉ N ₂ O ₃	1.9	163.0754, 171.1492	C ₁₀ H ₁₁ O ₂ , C ₉ H ₁₉ N ₂ O	-0.2, -0.3	7 (13.69%)	14 (2.94%)	-
M20	5.48	Hydroxylation (C)	303.2067	C ₁₈ H ₂₇ N ₂ O ₂	1.4	133.0648, 171.1492	C ₉ H ₉ O, C ₉ H ₁₉ N ₂ O	0.6, 0.8	13 (3.93%)	13 (3.18%)	-
M21	5.70	DIOH (C) + O-methylation	333.2173	C ₁₉ H ₂₉ N ₂ O ₃	0	163.0754, 171.1492	C ₁₀ H ₁₁ O ₂ , C ₉ H ₁₉ N ₂ O	1.9, 1.3	23 (072%)	-	-
M22	5.73		263.1754	C ₁₅ H ₂₃ N ₂ O ₂	0.7	131.1179, 133.0648	C ₆ H ₁₅ N ₂ O, C ₉ H ₉ O	0.3, 0.4	21 (0.9%)	25 (0.11%)	-

(Continues)

TABLE 1 (Continued)

ID	RT (min)	Biotransformation	Calculated [M + H] ⁺	Formula [M + H] ⁺	Mass error (ppm)	Diagnostic product ions (m/z)	Diagnostic product ions formula	Diagnostic product ions mass error (ppm)	Post-mortem urine ranking position (MAR %)	Post-mortem blood ranking position (MAR %)	pHLM ranking position (MAR %)
DIOH (C and P) + N-deacylation											
M23	5.89	Oxidation + N-deacylation	245.1648	C ₁₅ H ₂₃ N ₂ O ₂	-0.8	113.1073, 133.0648	C ₆ H ₁₃ N ₂ , C ₉ H ₉ O	-0.6, -0.3	10 (7.09%)	15 (2.83%)	9 (2.49%)
M24	6.10	Hydroxylation (P)	303.2067	C ₁₈ H ₂₇ N ₂ O ₂	1.4	117.0699, 185.1285	C ₉ H ₉ , C ₉ H ₁₇ N ₂ O ₂	1.3, 2	16 (2.68%)	8 (5.15%)	6 (3.92%)
M25	6.14	DIOH (C) + O-methylation	333.2173	C ₁₉ H ₂₉ N ₂ O ₃	1.3	163.0754, 171.1492	C ₁₀ H ₁₁ O ₂ , C ₉ H ₁₉ N ₂ O	0.5, -0.7	2 (84.45%)	3 (39.38%)	-
M26	6.39	Hydroxylation (C)	303.2067	C ₁₈ H ₂₇ N ₂ O ₂	0.7	133.0648, 171.1492	C ₉ H ₉ O, C ₉ H ₁₉ N ₂ O	0.7, 1.4	24 (0.7%)	-	-
M27	6.67	Hydroxylation (P) + N-deacylation	247.1805	C ₁₅ H ₂₃ N ₂ O	0.2	114.0913, 117.0699	C ₆ H ₁₃ N ₂ O, C ₉ H ₉ O	0.4, -0.5	5 (14.96%)	1 (100%)	1 (100%)
M28	7.02	DIOH (C and P)	319.2016	C ₁₈ H ₂₇ N ₂ O ₃	1.7	133.0648, 187.1441	C ₉ H ₉ O, C ₉ H ₁₉ N ₂ O ₂	0.7, 0.9	27 (0.41%)	-	11 (0.16%)
M29	7.03	Hydroxylation (P)	303.2067	C ₁₈ H ₂₇ N ₂ O ₂	1.4	117.0699, 185.1285	C ₉ H ₉ , C ₉ H ₁₇ N ₂ O ₂	0.9, -1.2	3 (32.6%)	5 (7.36%)	-
M30	9.35	O-methylation	317.2224	C ₁₉ H ₂₉ N ₂ O ₂	2.6	107.048, 147.0804	C ₇ H ₇ , C ₁₀ H ₁₆ O	1.1, 0.2	32 (0.16%)	16 (1.53)	-
M31	10.22	Hydroxylation (P) + N-deacylation	247.1805	C ₁₅ H ₂₃ N ₂ O	0.7	114.0913, 117.0699	C ₆ H ₁₃ N ₂ O, C ₉ H ₉ O	1.9, 0.2	26 (0.51%)	19 (1.04%)	-
M32	10.38	Hydroxylation (P)	303.2067	C ₁₈ H ₂₇ N ₂ O ₂	2.8	117.0699, 185.1285	C ₉ H ₉ , C ₉ H ₁₇ N ₂ O ₂	1.7, 3.4	14 (3.74%)	12 (3.48%)	3 (19.48%)

Abbreviations: A, acyl moiety; C, cinnamyl moiety; DIOH, dihydroxylation; P, piperazin moiety; pHLM, pooled human liver microsomes.

FIGURE 3 Postulated *in vivo* phase I biotransformation pathways of AP-238 as investigated in authentic urine samples. AP-238 and its most abundant metabolites are highlighted in green and yellow, respectively.

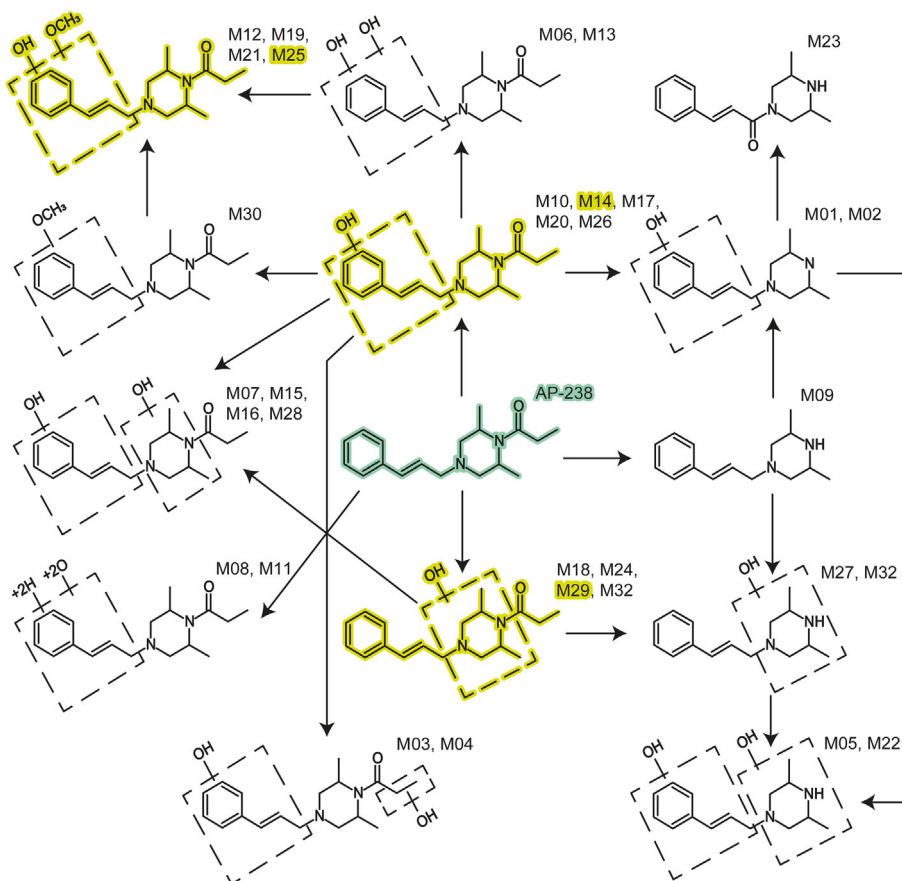
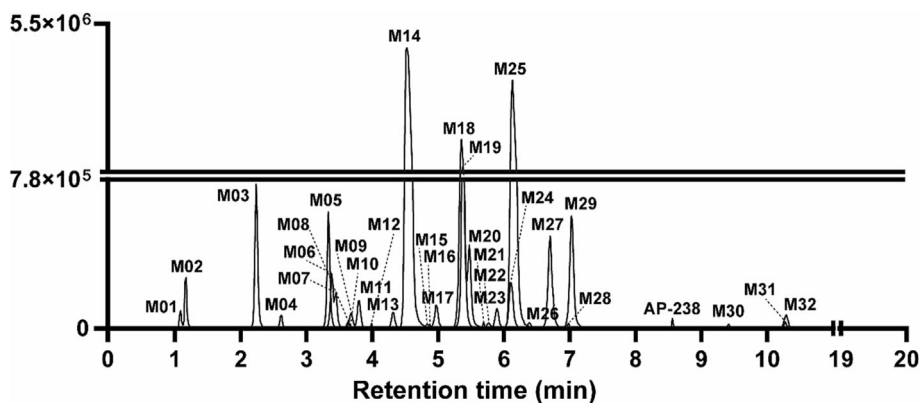


FIGURE 4 Extracted-ion chromatogram of AP-238 and metabolites in positive-ionization mode obtained from post-mortem urine (sample n°2). Mass tolerance, 5 ppm.



hydroxylation (+O), as indicated by the + 15.9949 Da mass shift from the parent. The fragment at m/z 133.0648 suggests that the biotransformation occurred at the cinnamyl moiety. Monohydroxylation at the phenyl ring was also found to be dominating in the metabolism of AP-237 in a study of Baba et al.²⁹ M10, M17, and M26 shared the same fragmentation pattern, while slight differences of intensity were observed for fragments at m/z 115.123 and at m/z 171.1492, piperazine and AP moieties, respectively, in the spectrum of M20. Interestingly, the fragment at m/z 105.0699, characteristic of a phenethyl cation, occurred in all of the above-mentioned metabolites' spectra,

preventing the determination of the exact location of hydroxylation within the cinnamyl moiety. It is well known that phenyl allyl cations can easily undergo intramolecular cyclization to the corresponding indanyl cations, with possible migration of functional groups.³⁰ Thus, the fragment at m/z 105.0699 could be generated after fragmentation of the indanyl cycle. However, under the present analytical conditions, the exact location of the hydroxylation in M10, M14, M17, M20, and M26 cannot be determined.

The hydroxylation at the AP moiety represented another frequent biotransformation pathway of AP-238, leading to the formation of the

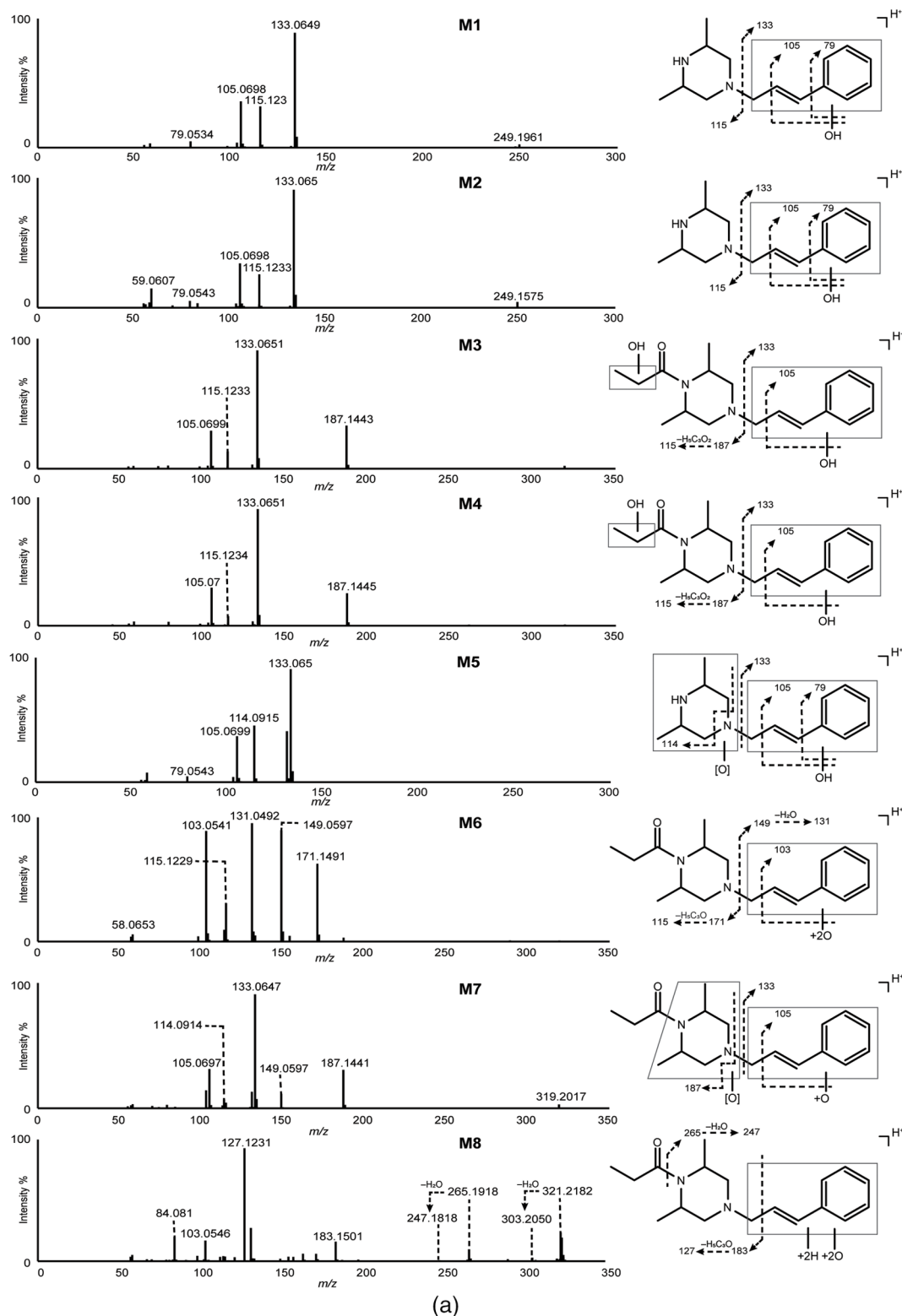
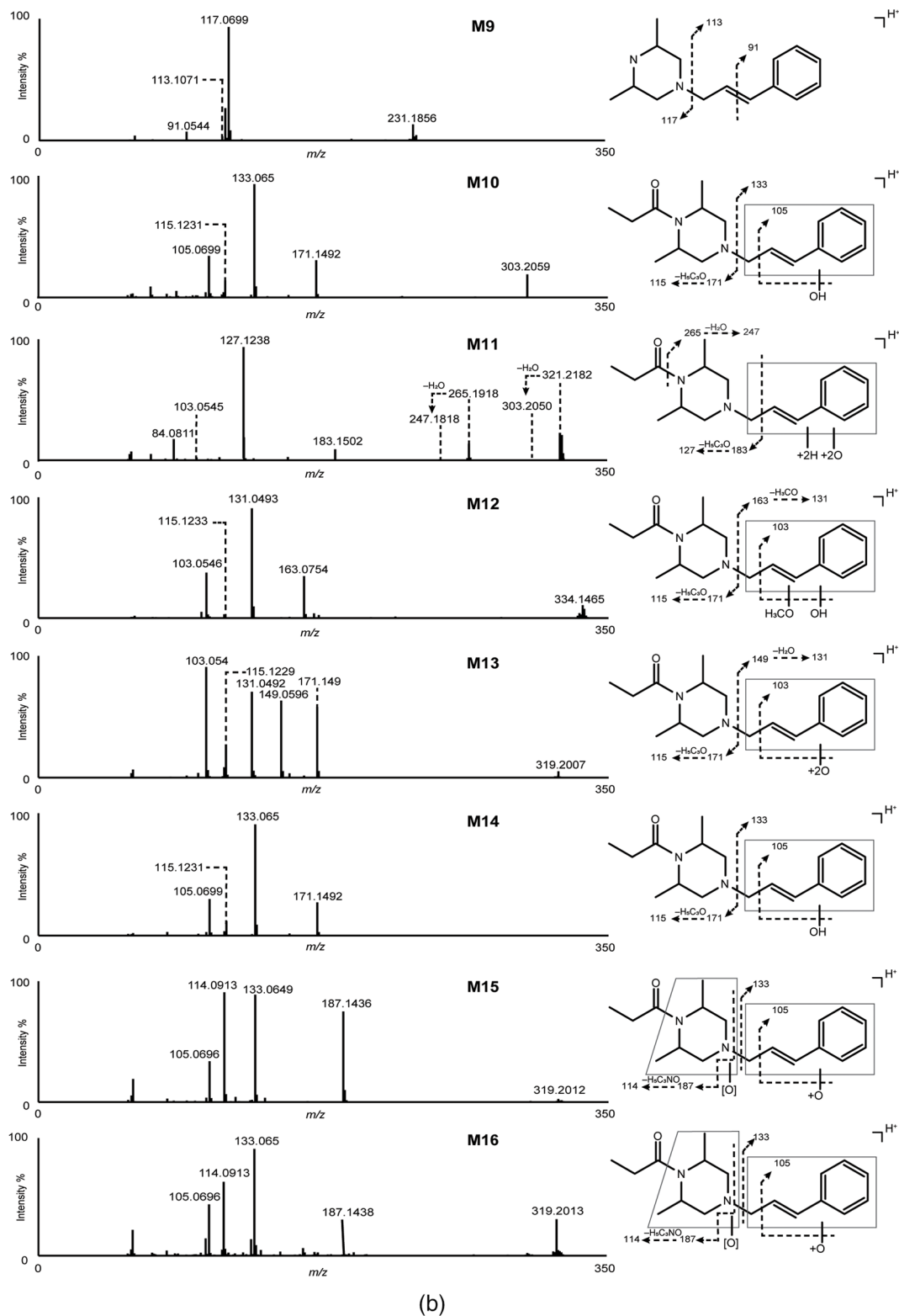


FIGURE 5 (a–d) LC-qToF-MS spectra (inclusion list) of AP-238's most abundant urinary metabolites, as observed in authentic urine specimens.

positional isomers M18, M24, M29, and M32. The detection of specific ion fragments at m/z 185.1285 and m/z 117.0699 and the absence of m/z 115.123 suggest the localization of the hydroxyl at the piperazine core. Once again, it is not possible to determine the

exact site of hydroxylation, although the late elution of M29 and M32 may indicate the presence of *N*-oxides.^{7,25,31} Taking into consideration the mean area ratios (MAR%), M29 was the third most abundant metabolite in urine and the fifth in blood.

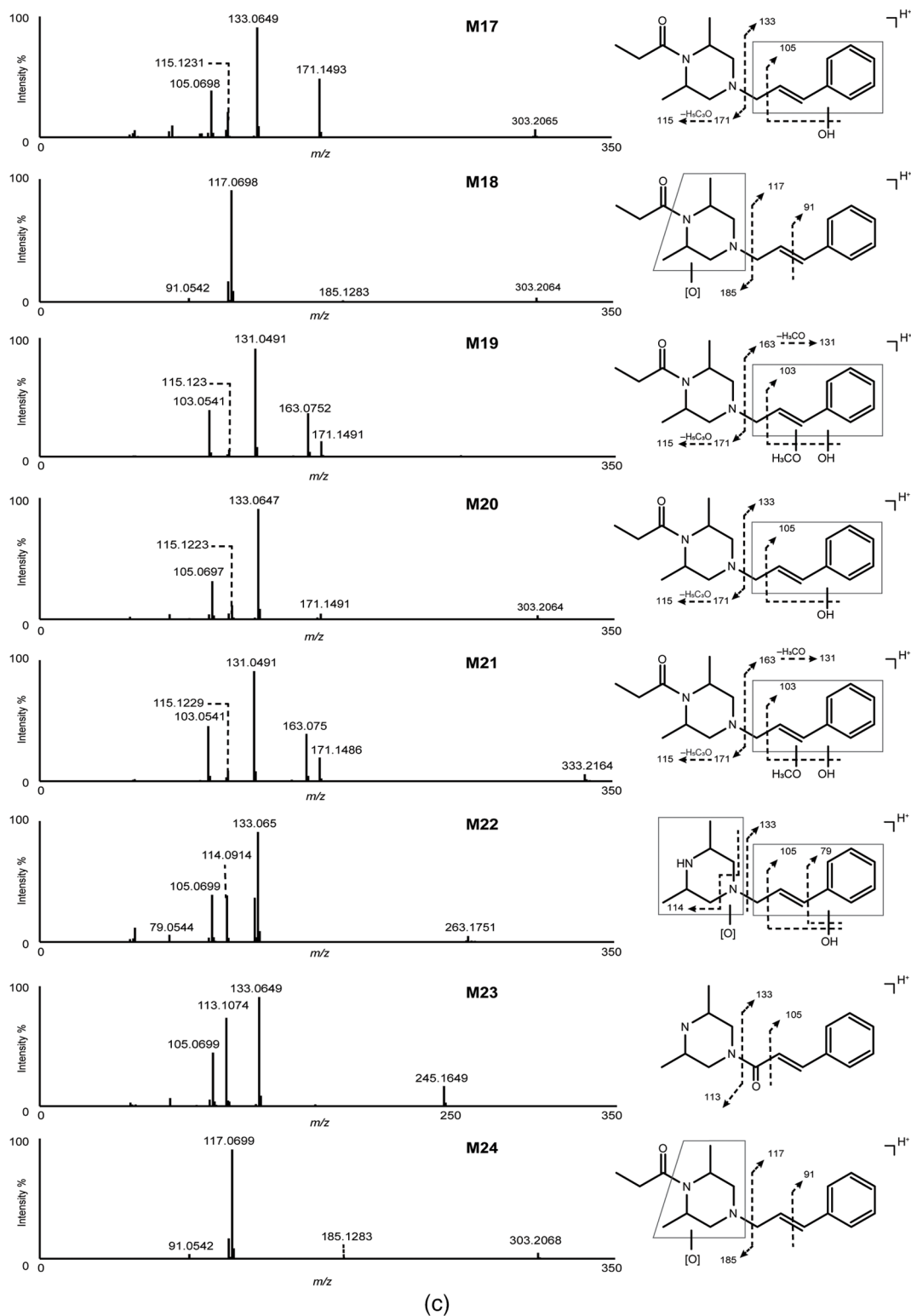


(b)

FIGURE 5 (Continued)

Eight dihydroxylated metabolites ($[\text{M} + \text{H}]^+$ at m/z 319.2016) were identified, characterized by a mass shift of 31.9898 Da (+2O) from the parent. The most dominant was M03, which, together with M04, was hydroxylated once at the cinnamyl moiety and once at the

acyclic portion, as suggested by the fragments at m/z 185.1285, m/z 115.123, and m/z 133.0648. The presence of the fragment at m/z 114.0913, characteristic of the hydroxylated 2,6-dimethylpiperazine cleavage, instead of that at m/z 115.123, allowed the identification



(c)

FIGURE 5 (Continued)

of M07, M15, M16, and M28 as dihydroxylated metabolites at the cinnamyl moiety and at the piperazine core. M06 and M13 can be interpreted as dihydroxylation of AP-238 at the cinnamyl moiety, as indicated by the fragments at m/z 149.0597.

3.1.2 | O-methylation

M12, M19, M21, and M25 ($[\text{M} + \text{H}]^+$ at m/z 333.2173) were generated after dihydroxylation and methylation of one of the hydroxyl

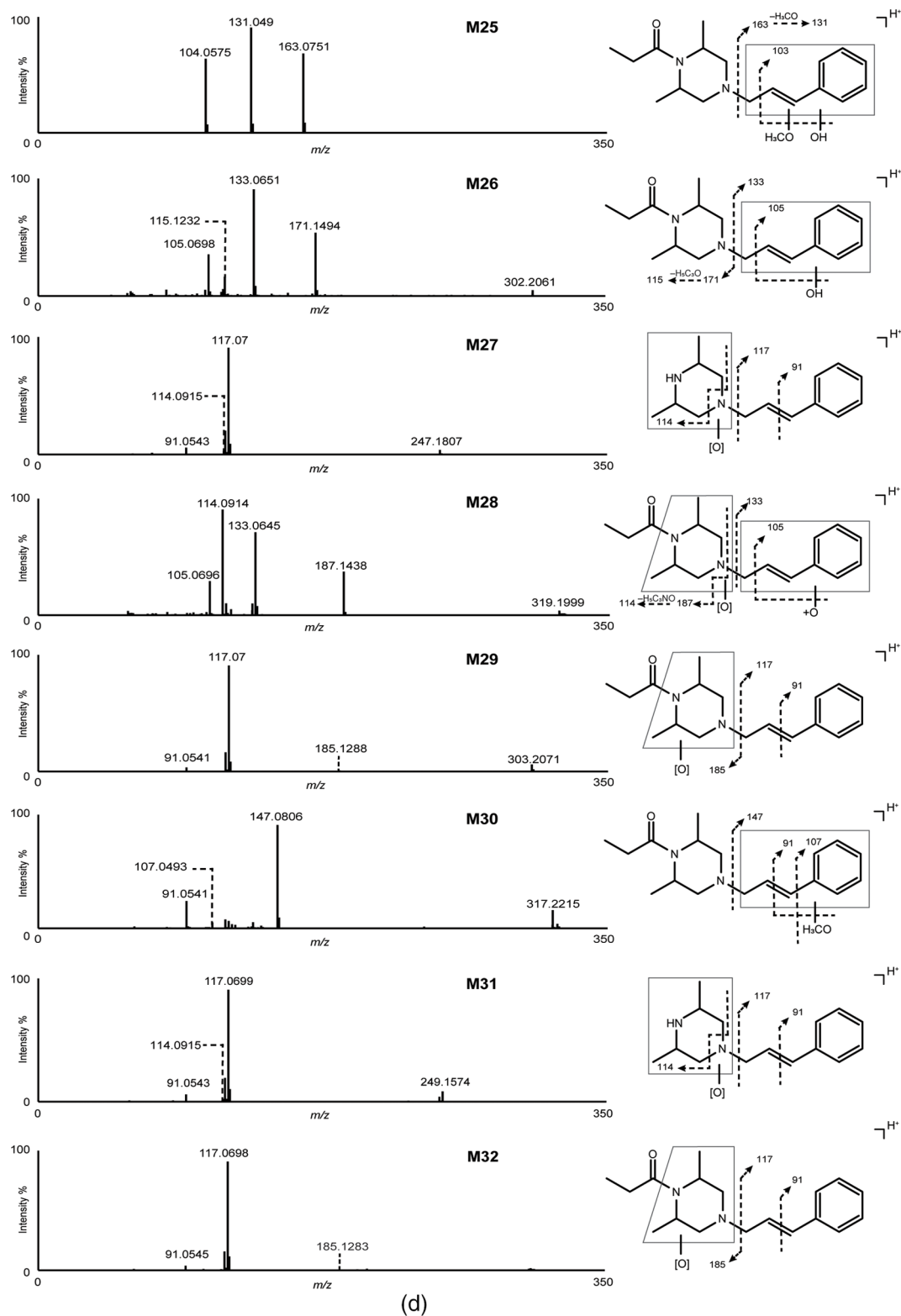


FIGURE 5 (Continued)

groups of the cinnamyl moiety, as indicated by the fragment at m/z 163.0754. The loss of the methoxy group led to the formation of the ion at m/z 131.0491. Remarkably, the most abundant metabolite

(M25) was characterized by a lower intensity of ions at m/z 115.123 and at m/z 171.1492 when compared with M12, M19, and M21. This suggests a difference in the location of these two substituents,

although their exact position cannot be determined from our data. In humans, the methylation of aromatic hydroxy groups is catalyzed by two different enzymes: catechol O-methyltransferase (COMT) and phenol O-methyltransferase (PMT). Mechanistically, a transfer of the methyl moiety from the co-factor S-adenosyl-methionine onto one of the aromatic hydroxyl groups was postulated.³² Since COMTs are responsible for the metabolism of catecholamines, it is likely that at least one of the metabolites M06 and M13 bears a catechol moiety, acting as an intermediate in the formation of M12, M19, M21, or M25. On the other hand, PMT could have also been responsible for the methylation of the phenolic groups of one or both of the above-mentioned cinnamyl-dihydroxylated metabolites, although this represents a minor metabolic pathway. Another possible way is represented by the hydroxylation of M30, the methoxy metabolite of AP-238. This minor metabolite might originate from one of the cinnamyl-hydroxylated metabolites ($[M + H]^+$ at m/z 303.2067) under the action of PMT, as indicated by the fragment at m/z 149.0804. Because PMT substrates are phenols, the methoxy group is suggested to be located at the benzene ring, as further confirmed by the ion at m/z 107.0491.

Because of the absence of S-adenosyl-methionine as a co-factor, all the metabolites in this section were not predicted by the pHLM assay.

3.1.3 | N-deacylation

M09 ($[M + H]^+$ at m/z 231.1856) emerged from the N-deacylation of the piperazine, as suggested by the -56.0262 Da mass shift from the parent. Its MS^2 spectrum was similar to that of AP-238, except for the characteristic fragment at m/z 169.1335. Following the same reasoning, there is a good chance that M01 and M02 originate from the metabolites bearing a hydroxyl at the cinnamyl moiety. M27 and M31, as well, can be interpreted as the N-deacyl N-oxides generated from M29 and M32, as suggested by their late elution. Similarly, M07, M15, M16, and M28 would plausibly be intermediates for the formation of their N-deacyl analogs, M05 and M22.

3.1.4 | Dihydrodiol formation

Benzenedihydrodiols are common metabolites of benzene-bearing substances and are formed via epoxidation and subsequent epoxide hydration.³³ M08 and M11 ($[M + H]^+$ at m/z 321.2173) are AP-238 dihydrodiol derivatives, as suggested by the $+34.0056$ Da mass shift from the parent. The water loss observed in their MS^2 spectra is extremely favorable for reestablishing the aromaticity of the ring. However, the cleavage between the α and the β carbons of the allyl moiety, which generates the fragments at m/z 183.1492 and at m/z 127.123, may indicate the presence of a proximal heteroatom. If the dihydrodiol formation involved the allylic double bond, it would be possible that M08 and M11 were the pair of diastereomers that originated after the formation of two asymmetric centers. Once again, unfortunately, it is impossible to determine the exact position of the two hydroxyl groups.

3.1.5 | Reduction and oxidation

Finally, M23 was a minor metabolite generated after oxidation of the hydroxyl group bound to the C1 of the phenyl allyl substituent. It is possible that M23 stems from an intermediate hydroxylated metabolite originating from M09 or after the oxidation of M01 and M02.

Comparing these results to a metabolic study of AP-237 by Morishita et al., the vast majority of metabolic transformations that occurred were consistent with the metabolic profile of AP-238.³⁴

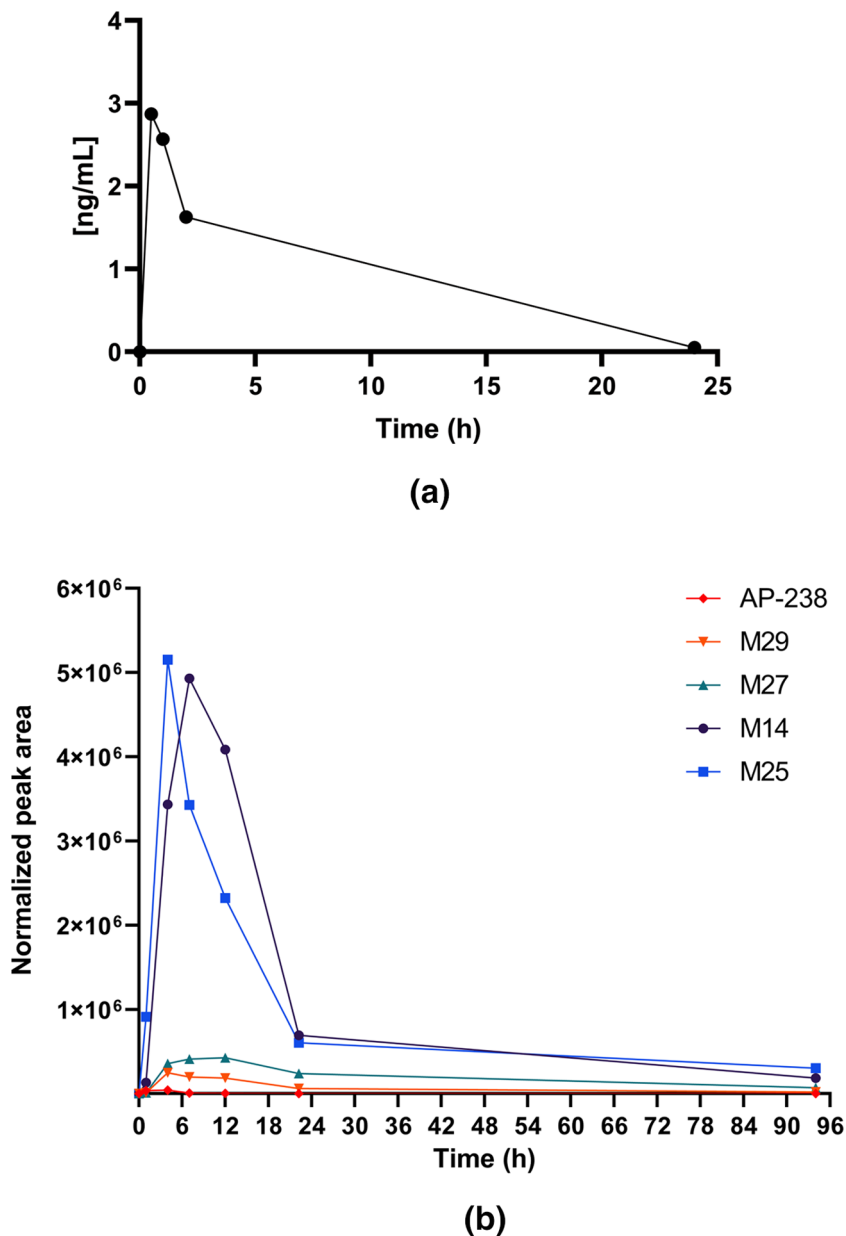
3.2 | Serum concentrations and metabolic profile in urine after AP-238 self-administration

Data on the basic pharmacokinetic properties of new compounds are important for assessing death cases and facilitating the interpretation of findings in abstinence control. The findings in blood and urine are graphically demonstrated in Figure 6a,b. After oral uptake, the peak concentration in serum of AP-238 was reached after 30 min (2.87 ng/mL), gradually decreasing 1 h (2.57 ng/mL) and 2 h (1.63 ng/mL) post-ingestion, displaying a relatively rapid gastrointestinal absorption, in line with the studies of Carrano et al. for AP-237.^{16,17} Twenty-four hours post-intake, the AP-238 serum concentration was below the range of calibration ($<LOQ$, Figure 6a). The volunteer did not experience any physical or mental impairment during the study. Considering the relatively low dose ingested, this was not surprising.

To prove the uptake of illicit drugs, urine is often the preferred biological matrix for forensic and clinical toxicology, particularly in drug abstinence testing when longer detection windows are needed.³⁵ For this purpose, six urine samples obtained after the self-administration of AP-238 were submitted to qualitative analysis using LC-QToF-MS. Inclusion criteria listed in Section 2.5 were applied, and peak areas were normalized for the creatinine values (Figure 6b). Only traces of unmetabolized AP-238 were detected in urine, starting from the sample obtained at 50 min up to the sample collected 21 h and 20 min post-ingestion. Metabolites M14, M25, M27, and M29 could be detected in the urine samples obtained between 50 min and 94 h post-ingestion. For abstinence control, monitoring these four specific metabolites in urine is recommended.

Remarkably, although it was assigned rank #2 in the post-mortem urine metabolism study (Table 1), M25 was the most dominant metabolite for the first 3 h after being temporarily displaced by M14 (rank #1 in Table 1), which reached a maximum of 5 h 40 min post-ingestion. This might be a starting point for estimation of the time that passed between consumption and death in post-mortem cases, although it has to be mentioned that dose, route of administration, and other variables would have to be considered for a valid interpretation. It has to be kept in mind that NSOs are often consumed by injecting, smoking, or nasal insufflation and not by oral administration.³⁶ Parenteral intake could thus result in stronger effects at the same dose and different kinetic profiles.

FIGURE 6 (a) Serum concentrations (30 min, 1, 2, and 24 h post intake) received by LC-MS/MS analysis of samples obtained after a single oral administration of 1.19 mg AP-238 HCl to a human volunteer. (b) Peak areas for AP-238 and main metabolites M14, M25, M27, and M29 were detected after conjugate cleavage in six urine samples after 30 min, 1, 4, 7, 23, and 96 h of self-administration of 1.19 mg AP-238 HCl to a human volunteer. All values were normalized to a creatinine concentration of 100 mg/dL.



3.3 | Limitations

Several isomeric metabolites with the same MS² spectra but different retention times were detected after the biotransformation of AP-238. To clearly identify the location of the functional groups introduced by metabolic reactions, the synthesis of reference material or the isolation of the metabolites of interest for structure elucidation, for example by NMR spectroscopy, would be required. Thus, in the present study, it was not possible to elucidate the exact chemical structures of the majority of the metabolites.

As a second limitation, the *in vivo* MAR% were based on the chromatographic peak areas and might not accurately reflect absolute concentrations, given possible differences in ionization efficiency and matrix effects. Matrix effects were also not evaluated for the semi-quantitative determination of AP-238 in serum.

Third, additional phase II metabolites could be found in authentic samples when omitting the enzymatic cleavage step with β -glucuronidase/arylsulfatase or when assays based on hepatocytes, pHLS9, or animal models are performed. However, as routine analysis usually involves a hydrolysis step, phase I metabolites are preferred, and the vast portfolio of specific biomarkers identified is more than sufficient to prove the uptake of AP-238.

4 | CONCLUSIONS

The occurrence of NSOs, and particularly AP opioids, as a replacement of FAs is of rising concern. Developing analytical methods for the detection of their metabolites is extremely important to correctly assign the cause of intoxication in clinical cases or death cases and to

complement analytical strategies for abstinence control. In the present study, the in vitro and in vivo metabolism of AP-238 was investigated using a pHLM assay, samples from death cases, and samples from a controlled oral self-administration experiment, resulting in the detection of a total of 32 metabolites. Among the detected metabolites, particularly hydroxylated AP-238 (M14, M29), dihydroxylated and O-methylated AP-238 (M25), and N-deacylated and hydroxylated AP-238 (M27) can be recommended as biomarkers to be monitored in abstinence screening due to their relatively high abundance.

ORCID

Pietro Brunetti  <https://orcid.org/0000-0001-5271-7773>

Hannes Max Schwelm  <https://orcid.org/0000-0001-7867-5831>

Belal Haschimi  <https://orcid.org/0000-0003-2954-7539>

Volker Auwärter  <https://orcid.org/0000-0002-1883-2804>

REFERENCES

- Gampfer TM, Wagmann L, Park YM, et al. Toxicokinetics and toxicodynamics of the fentanyl homologs cyclopropanoyl-1-benzyl-4'-fluoro-4-anilinopiperidine and furanoyl-1-benzyl-4-anilinopiperidine. *Arch Toxicol.* 2020;94(6):2009-2025. doi:10.1007/s00204-020-02726-1
- Giorgetti A, Brunetti P, Pelotti S, Auwärter V. Detection of AP-237 and synthetic cannabinoids on an infused letter sent to a German prisoner. *Drug Test Anal.* 2022;14(10):1779-1784. doi:10.1002/dta.3351
- EMCCDA. Spotlight on ... Fentanils and other new opioids. Accessed August 24, 2022. https://www.emccda.europa.eu/spotlights/fentanils-and-other-new-opioids_en
- EMCCDA. European Drug report 2022: Trends and developments. Accessed August 24, 2022. <https://www.emccda.europa.eu/system/files/publications/14644/TDAT22001ENN.pdf>
- Lamy FR, Daniulaityte R, Barratt MJ, Lokala U, Sheth A, Carlson RG. "Etazene, safer than heroin and fentanyl": non-fentanyl novel synthetic opioid listings on one darknet market. *Drug Alcohol Depend.* 2021;225:108790. doi:10.1016/j.drugalcdep.2021.108790
- Vandeputte MM, Cannart A, Stove CP. In vitro functional characterization of a panel of non-fentanyl opioid new psychoactive substances. *Arch Toxicol.* 2020;94(11):3819-3830. doi:10.1007/s00204-020-02855-7
- Grafinger KE, Wilde M, Otte L, Auwärter V. Pharmacological and metabolic characterization of the novel synthetic opioid brophine and its detection in routine casework. *Forensic Sci Int.* 2021;327:110989. doi:10.1016/j.forsciint.2021.110989
- Pardo B, Taylor J, Caulkins J, Reuter P, Kilmer B. The dawn of a new synthetic opioid era: the need for innovative interventions. *Addiction.* 2021;116(6):1304-1312. doi:10.1111/add.15222
- Clinton HA, Thangada S, Gill JR, Mirizzi A, Logan SB. Improvements in toxicology testing to identify fentanyl analogs and other novel synthetic opioids in fatal drug overdoses, Connecticut, January 2016–June 2019. *Public Health Rep.* 2021;136(1_suppl):80S-86S. doi:10.1177/003335492111042829
- UNODC. World Drug Report 2021. Booklet 3. Accessed April 22, 2022. https://www.unodc.org/res/wdr2021/field/WDR21_Booklet_3.pdf
- Di Trana A, Pichini S, Pacifici R, Giorgetti R, Busardò FP. Synthetic Benzimidazole opioids: the emerging health challenge for European drug users. *Front Psych.* 2022;13:858234. doi:10.3389/fpsy.2022.858234
- EMCCDA. New psychoactive substances: global markets, global threats and the COVID-19 pandemic. https://www.emccda.europa.eu/system/files/publications/13464/20205648_TD0320796ENN_PDF_rev.pdf
- De Baerdemaeker KSC, Dines AM, Hudson S, et al. Isotonitazene, a novel psychoactive substance opioid, detected in two cases following a local surge in opioid overdoses. *QJM Mon J Assoc Phys.* 2022; 116(2):hcac039. doi:10.1093/qjmed/hcac039
- Krotulski A, Mohr ALA, Logan BK. Trend Report: Q2 2021–NPS Opioids in the United States. 2021 Accessed June 22, 2022. https://www.cfsre.org/images/trendreports/2021-Q2_NPS-Opioids_Trend-Report.pdf
- Krotulski A, Mohr ALA, Logan BK. Trend Report: Trend Report: Q3 2022 NPS Opioids in the United States. Accessed December 8, 2022. <https://www.cfsre.org/images/trendreports/2022-Q3-NPS-Opioids-Trend-Report.pdf>
- Carrano RA, Kimura KK, Landes RC, McCurdy DH. General pharmacology of a new analgesic-AP-237. *Arch Int Pharmacodyn Ther.* 1975; 213(1):28-40.
- Carrano RA, Kimura KK, McCurdy DH. Analgesic and tolerance studies with AP-237, a new analgesic. *Arch Int Pharmacodyn Ther.* 1975; 213(1):41-57.
- Irikura T, Masuzawa K, Nishino K, et al. New analgesic agents. V. 1-butyl-4-cinnamylpiperazine hydrochloride and related compounds. *J Med Chem.* 1968;11(4):801-804. doi:10.1021/jm00310a022
- Resnik K, Brandão P, Alves EA. DARK classics in chemical neuroscience: Bucinnazine. *ACS Chem Neurosci.* 2021;12(19):3527-3534. doi:10.1021/acscchemneuro.1c00522
- Zhang C, Han SQGW, Zhao H, Lin S, Hasi WLJ. Detection and quantification of Bucinnazine hydrochloride injection based on SERS technology. *Anal Sci Int J Jpn Soc Anal Chem.* 2018;34(11):1249-1255. doi:10.2116/analsci.18P158
- Krotulski A, Fogarty M, Papsun D, Logan BK. AP-238 Monograph. Accessed August 25, 2022. https://www.cfsre.org/images/monographs/AP-238_111120_CFSRE_Toxicology_Report.pdf
- EMCCDA. EDND. Accessed April 22, 2022. <https://ednd2.emccda.europa.eu/ednd/substanceProfiles/1010>
- Cignarella G, Testa E. 2,6-Dialkylpiperazines. IV. 1-Propionyl-4-substituted cis-2,6-dimethylpiperazines structurally related to the analgesic 8-acyl-3,8-diazabicyclo[3.2.1]octanes. *J Med Chem.* 1968; 11(3):592-594. doi:10.1021/jm00309a039
- Fogarty MF, Vandeputte MM, Krotulski AJ, et al. Toxicological and pharmacological characterization of novel cinnamylpiperazine synthetic opioids in humans and in vitro including 2-methyl AP-237 and AP-238. *Arch Toxicol.* 2022;96(6):1701-1710. doi:10.1007/s00204-022-03257-7
- Watanabe S, Vikingsson S, Roman M, Green H, Kronstrand R, Wohlfarth A. In vitro and in vivo metabolite identification studies for the new synthetic opioids Acetylfentanyl, Acrylfentanyl, Furanylfentanyl, and 4-Fluoro-Isobutyrylfentanyl. *AAPS J.* 2017;19(4):1102-1122. doi:10.1208/s12248-017-0070-z
- Giorgetti A, Brunetti P, Haschimi B, Busardò FP, Pelotti S, Auwärter V. Human phase-I metabolism and prevalence of two synthetic cannabinoids bearing an ethyl ester moiety: 5F-EDMB-PICA and EDMB-PINACA. *Drug Test Anal.* 2022;15(3):299-313. doi:10.1002/dta.3405
- Hassanien SH, Layle NK, Holt MC, Zhao T, Iula DM. Cayman NPS Metabolism Monograph <https://cdn2.caymanchem.com/cdn/cms/caymanchem/LiteratureCMS/2-methyl%20AP-237%20Metabolomics%20Monograph.pdf>
- Huppertz LM, Moosmann B, Auwärter V. Flubromazolam—basic pharmacokinetic evaluation of a highly potent designer benzodiazepine. *Drug Test Anal.* 2018;10(1):206-211. doi:10.1002/dta.2203
- Baba S, Morishita S. Studies on drug metabolism by use of isotopes. XVI. Species differences in metabolism of 1-butyl-4-cinnamylpiperazine hydrochloride. *Chem Pharm Bull(Tokyo).* 1975; 23(9):1949-1954. doi:10.1248/cpb.23.1949

30. Olah GA, Asensio G, Mayr H. 1-Phenylallyl cations and their rearrangement to indanyl cations in superacidic media. *J Org Chem.* 1978; 43(8):1518-1520. doi:[10.1021/jo00402a006](https://doi.org/10.1021/jo00402a006)
31. Di Trana A, Brunetti P, Giorgetti R, et al. In silico prediction, LC-HRMS/MS analysis, and targeted/untargeted data-mining workflow for the profiling of phenylfentanyl in vitro metabolites. *Talanta.* 2021; 235:122740. doi:[10.1016/j.talanta.2021.122740](https://doi.org/10.1016/j.talanta.2021.122740)
32. Weinshilboum R. Pharmacogenetics of methylation: relationship to drug metabolism. *Clin Biochem.* 1988;21(4):201-210. doi:[10.1016/s0009-9120\(88\)80002-x](https://doi.org/10.1016/s0009-9120(88)80002-x)
33. Brunetti P, Lo Faro AF, Di Trana A, et al. β '-Phenylfentanyl metabolism in primary human hepatocyte incubations: identification of potential biomarkers of exposure in clinical and forensic toxicology. *J Anal Toxicol.* 2022;46(9):bkac065. doi:[10.1093/jat/bkac065](https://doi.org/10.1093/jat/bkac065)
34. Morishita SI, Baba S, Nagase Y. Studies on drug metabolism by use of isotopes XX: ion cluster technique for detection of urinary metabolites of 1-butyryl-4-cinnamylpiperazine by mass chromatography. *J Pharm Sci.* 1978;67(6):757-761. doi:[10.1002/jps.2600670606](https://doi.org/10.1002/jps.2600670606)
35. Concheiro M, Chesser R, Pardi J, Cooper G. Postmortem toxicology of new synthetic opioids. *Front Pharmacol.* 2018;9:1210. doi:[10.3389/fphar.2018.01210](https://doi.org/10.3389/fphar.2018.01210)
36. Pérez-Mañá C, Papaseit E, Fonseca F, Farré A, Torrens M, Farré M. Drug interactions with new synthetic opioids. *Front Pharmacol.* 2018; 9:1145. doi:[10.3389/fphar.2018.01145](https://doi.org/10.3389/fphar.2018.01145)

SUPPORTING INFORMATION

Additional supporting information can be found online in the Supporting Information section at the end of this article.

How to cite this article: Brunetti P, Berardinelli D, Giorgetti A, et al. Human metabolism and basic pharmacokinetic evaluation of AP-238: A recently emerged acylpiperazine opioid. *Drug Test Anal.* 2023;1-15. doi:[10.1002/dta.3535](https://doi.org/10.1002/dta.3535)